NSTX FY2009 Year End Report

NSTX successfully completed its FY 2009 plasma campaign on August 14, 2009. NSTX met or exceeded all its research and facility/diagnostic milestones including the ARRA extended five run weeks. NSTX achieved a total of 16.84 run weeks (target - 16 run weeks) with 2748 plasma shots, the most plasma shots per year with the highest plasma shot efficiency of 94.7%. The NSTX research team conducted over 50 experimental and machine proposals utilizing new capabilities including HHFW upgrades, dual lithium powder dropper, CHI absorber coils, a sample probe, and NBI feedback capability.

In FY2009, the NSTX research team successfully executed experiments in support of the 2009 DOE Joint milestone: "*Conduct experiments on major fusion facilities to develop understanding of particle control and hydrogenic fuel retention in tokamaks. In FY09, FES will identify the fundamental processes governing particle balance by systematically investigating a combination of divertor geometries, particle exhaust capabilities, and wall materials. Alcator C-mod operates with high-Z metal walls, NSTX is pursuing the use of lithium surfaces in the divertor, and DIII-D continues operating with all graphite walls. Edge diagnostics measuring the heat and particle flux to walls and divertor surfaces, coupled with plasma profile data and material surface analysis, will provide input for validating simulation codes. The results achieved will be used to improve extrapolations to planned ITER operation.*" The NSTX contributions to the 2009 Joint Research Milestone are described in a separate report.

Summary descriptions of the results of research, facility, and diagnostic milestones are provided below. Descriptions of other selected research highlights are also provided. Other NSTX information and statistics such as publications, invited talks, colloquium presentations, awards, and leadership are reported through the overall PPPL statistics.

Research Milestone R(09-1) Understand the physics of RWM stabilization and control as a function of rotation. (Target - September 2009. Completed – September 2009)

Milestone Description: NSTX experiments during FY2006 demonstrated active stabilization of the resistive wall mode at low rotation. The experiments revealed the important roles of the ion collisionality and the details of the plasma rotation profile in RWM stabilization. In FY2009, the RWM stabilization mechanisms will be characterized over a wide range of plasma conditions at rotation Mach numbers up to 0.8 using non-resonant field control. These experiments will allow comprehensive comparisons with theory to develop the physics of RWM stabilization. Understanding this physics at various levels of plasma rotation and collisionality will enable reliable projections of the RWM stabilization requirements to burning plasma devices with low rotation (e.g. ITER) as well as devices with high rotation (e.g. KSTAR, JT-60SA, CTF). Plasma rotation is anticipated to strongly affect plasma stability and confinement and, hence, the overall performance of these devices.

Milestone R(09-1) Report:

Recent research on the Resistive Wall Mode (RWM) has shown that kinetic effects are particularly important for determining the plasma rotation required to stabilize the RWM. Kinetic effects in general include (among others) resonances with trapped and passing ion and electron orbit motion, diamagnetic drift, bounce precession, and E×B drift motion. NSTX research in FY2009 focused on extending the physics of these phenomena to include the influence of fast-ions on RWM stability. Numerical calculations of the influence of fast-ions on RWM stability have been performed with the MISK code which computes the perturbed mode energy δW including kinetic effects using the unperturbed ideal kink eigen-function from the PEST code. Figure 1a shows a range of fast-ion pressure profiles scaled between 0 and 1 times the experimental value as computed with the TRANSP code to assess the effect of fast-ion pressure on RWM stability with other plasma parameters held fixed. As seen in Figure 1b, the RWM is predicted to become progressively more stable as the fast-ion pressure is increased – although some saturation in the growth rate is observed near a pressure scaling between 0.8 and 1 times the experimental value. From these calculations it is expected that fast-ion content from neutral beam injection (NBI) could strongly modify RWM stability in NSTX.

To test these predictions, dedicated experiments were performed in NSTX varying the fast-ion content by varying the plasma current and field at fixed edge safety factor q_{95} to vary the plasma temperature and density to change the fast-ion slowing down-time. Figure 2a shows the NBI fast-ion density profiles from the Fast-Ion D-alpha (FIDA) diagnostic for two different plasma conditions with the same global q_{95}. As seen in the

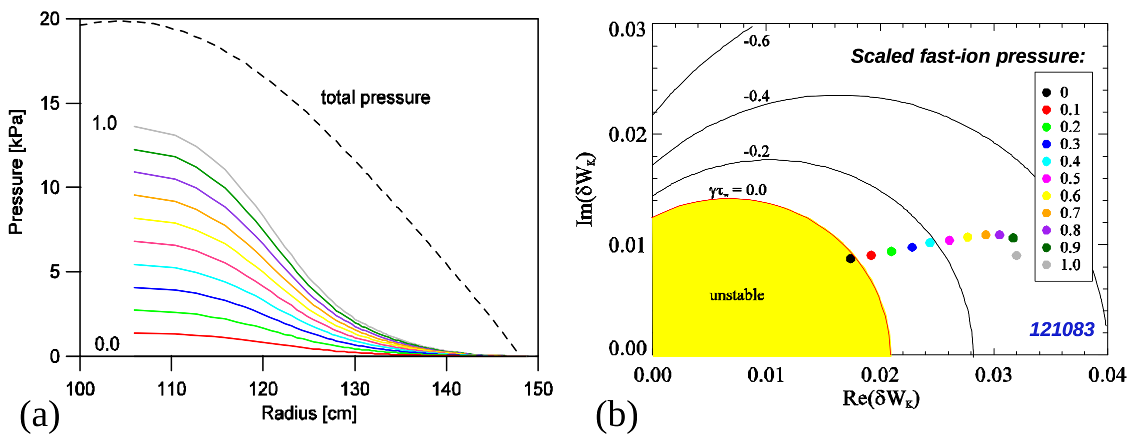

__Figure 1__ - (a) Scaled fast-ion pressure profiles from TRANSP for shot 121083 to be used in MISK stability analysis of the RWM, and (b) mode growth rate normalized to the resistive wall time as a function of fast-ion pressure scaling plotted in the imaginary vs. real $\delta W_{kinetic}$ plane.

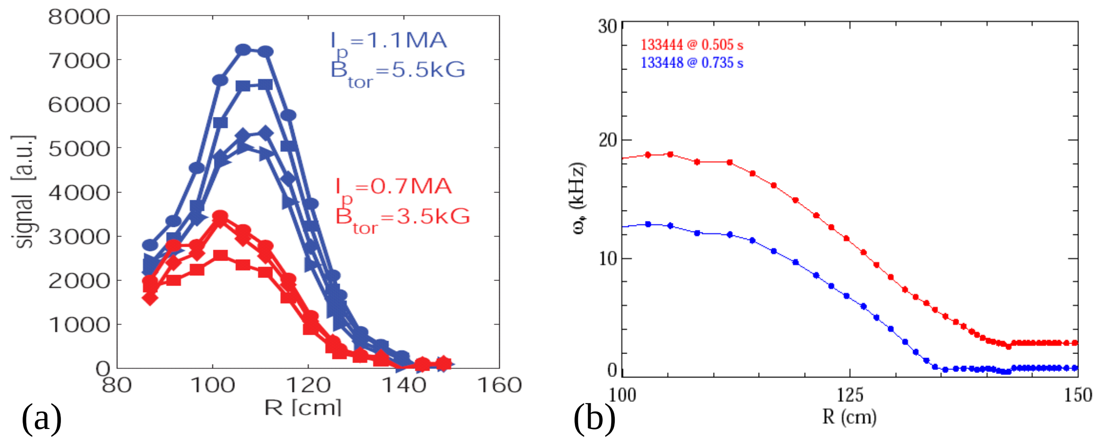

Figure 2 *- (a) Fast-ion density profiles from NBI as measured with the Fast-Ion D-alpha (FIDA) diagnostic for two different plasma currents at fixed q, and (b) plasma rotation profiles at RWM marginal stability for the fast-ion density conditions in (a).*

figure, the fast-ion content is significantly reduced for the plasma with lower field and current (and hence confinement and temperature) – consistent with decreased plasma slowing down time and reduced fast-ion content. As shown in Figure 2b, higher plasma rotation frequency is required to achieve RWM marginal stability for the plasma with lower fast ion content – consistent with theoretical predictions that fast-ions are stabilizing for the RWM. More detailed comparisons between measured and predicted stability thresholds are ongoing.

Research Milestone R(09-2) Study how j(r) is modified by super-Alfvénic ion driven modes. (Target - September 2009. Completed – September 2009)

Milestone Description: This research aims to determine the effects of MHD modes driven by the super-Alfvénic ions from neutral beam injection on the neutral beam driven current profiles, which can be a major component of the total current profile in NSTX. Results from FY2006 suggested that the effects of these modes can extend the durations over which *q(0)*, the safety factor at the magnetic axis of the plasma, can remain above 1. In this research the redistribution of the super-Alfvénic ions in the presence of Alfvén modes will be measured spectroscopically as a function of the measured Alfvén mode amplitude and spatial localization driven by these fast ions. Simultaneously, the plasma current and safety factor profiles will be determined using Motional Stark Effect (MSE) measurements of the pitch angle of the magnetic field and the measured plasma temperature, density, and rotation profiles to constrain the MHD equilibrium reconstruction. The resulting profile of the total toroidal plasma current will be compared to that modeled using neoclassical transport theory and classical slowing of the beam ions. Alfvén modes driven by the measured fast ion distributions will also be calculated to compare with the measured mode amplitudes and locations. This research will enable more realistic predictions of the effects in ITER and CTF of the copious super-Alfvénic fusion alpha particles on the destabilization of Alfvénic modes and the efficiency of plasma self-heating.

Milestone R(09-2) Report:

Fast-ion transport resulting from the wave-particle interaction between multiple simultaneous Alfvén-Eigenmode (AE) instabilities and the NBI fast-ion population (commonly called an "avalanche") is an important process that could impact the fusion performance of next-step STs and ITER burning plasmas. In FY2009, NSTX extended previous studies of fast-ion redistribution and loss to explore the effects of fast-ion transport on the equilibrium current profile evolution. Figure 3a shows time histories of plasma current, NBI heating power, and neutron rate for plasmas unstable to Beta-induced Alfvén-Acoustic Eigenmode (BAAE) instabilities. As shown in the bottom plot

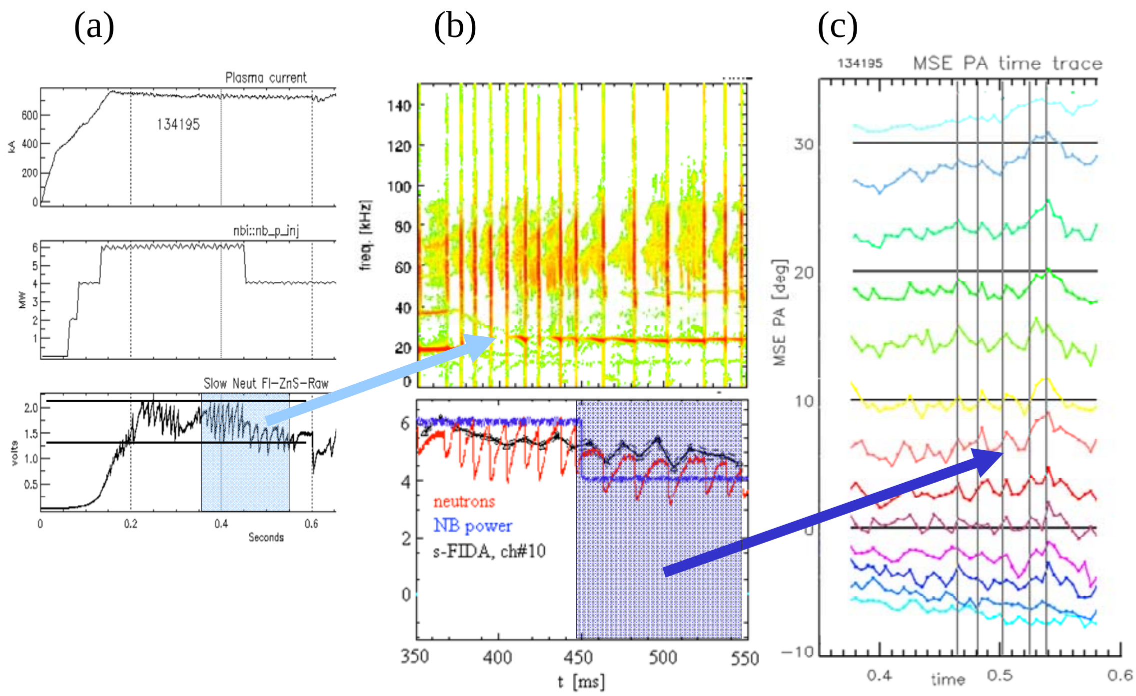

***Figure 3** - (a) Plasma current, NBI power, and neutron rates for plasmas with BAAE avalanches, (b) MHD mode spectrum of BAAE instabilities and comparison of neutron rate and FIDA signal, and (c) magnetic field pitch angle evolution measured with MSE during BAAE activity.*

of Figure 3a, there are large (up to ~30%) variations in the neutron rate associated with the BAAE activity. For the light blue shaded region of Figure 3a, Figure 3b shows that the drops in neuton rate (lower plot) correlate with times of maximum magnetic fluctuation amplitude as indicated by the red vertical lines on the magnetic fluctuation spectrogram (upper plot of 3b). In these experiments the size and occurrence frequency of BAAE burst events is reduced by reducing the NBI heating power as indicated by the dark blue shaded region on the bottom plot of Figure 3b. As a result of this reduced BAAE event frequency, the time-dependent modifications to the magnetic field pitch angle as measured by the Motional Stark Effect (MSE) diagnostic can be resolved for each event as shown in Figure 3c. These data are being used in MSE-constrained equilibrium reconstructions to assess the variation in current profile from each event, and will be used to determine through additional TRANSP modeling using resistive diffusion models of the current profile, the long-time-scale modification of the equilibrium current density profile from many BAAE avalanche events.

Research Milestone R(09-3) Perform high-elongation wall-stabilized plasma operation. (Target - September 2009. Completed – September 2009)

Milestone Description: Conditions will be studied on NSTX in which the toroidal plasma current is maintained for durations longer than the plasma current redistribution time using available current drive methods. The plasma elongation κ will be increased to increase the safety factor q. The expected positive scaling of the neoclassical bootstrap current fraction with increased q will be assessed, and wall-stabilization will also be utilized to prevent the development of pressure-driven instabilities. Strong neutral-beam injection (NBI) will be applied in low density plasmas, obtained using such techniques as lithium wall coating developed during FY2006–2008. This will increase the fraction of current driven by the NBI towards that anticipated in CTF. Discharges have already been produced in NSTX in which the solenoid-induced loop voltage has been reduced to the range 0.1 - 0.2 V for durations much longer than the current redistribution time. This was achieved by a combination of optimizing the current ramp-up, an early transition to the H-mode and strong plasma shaping to increase plasma stability and to minimize the impact of ELMs. Possible synergistic effects between the current drive mechanisms, such as current profile modification by super-Alfvénic-ion driven modes described in Milestone R(09-2), will be investigated to determine the optimal plasma scenarios. Simulation codes, which will have been benchmarked through comparison with NSTX data, will be used to identify combinations of techniques to produce long-pulse plasmas in conditions relevant to CTF.

Milestone R(09-3) Report:

NSTX scenario integration experiments in FY2009 focused on two operational goals important for ST development and the viability of next-step STs: (1) sustaining a high fraction of non-inductive current drive, and (2) sustaining high toroidal beta values. For high non-inductive fraction plasmas, high plasma elongation κ = 2.6-2.7 was sustained for the entire flat-top duration in an effort to increase the global safety factor and poloidal beta. Evaporated lithium coating of the plasma-facing components using the LITERs was used to help reduce the early plasma density and minimize or eliminate ELMs. Figure 4a shows that in these plasmas a high fraction of non-inductive current (~65%) is sustained for 800-900ms. This corresponds to 2.5 - 3 current redistribution times, which

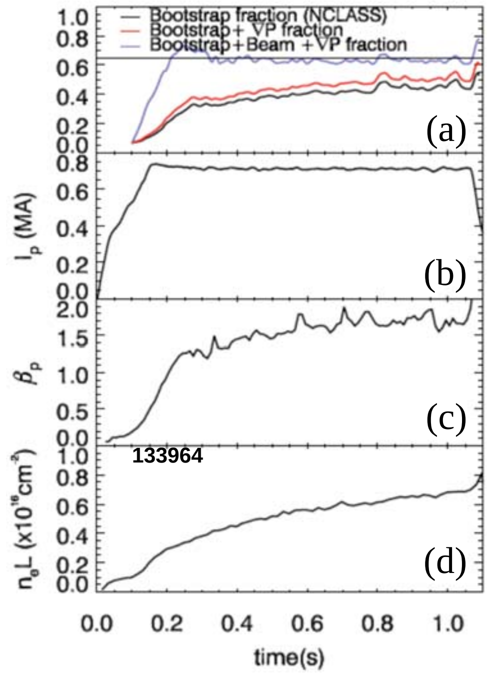

Figure 4 *- (a) Non-inductive current fraction, (b) total current, (c) poloidal beta, and (d) line-integrated density.*

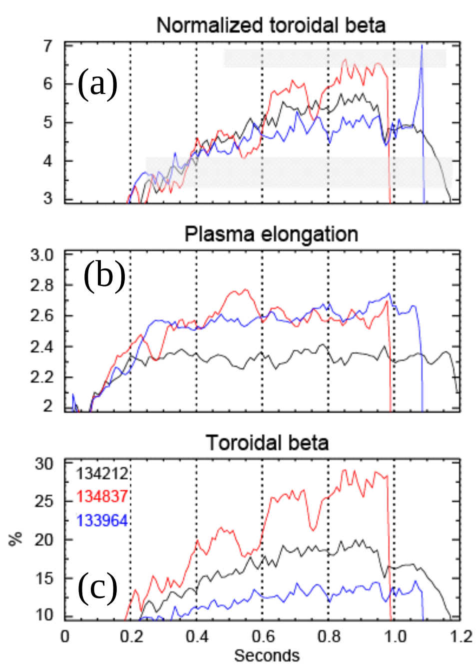

Figure 5 *- (a) Normalized beta, (b) elongation, (c) toroidal beta for a range of plasma currents I_P = 0.7-1.05MA and toroidal field B_T=0.48-0.41T.*

is 2 - 3 times longer than sustained in previous high non-inductive current fraction NSTX plasmas.

A noteworthy characteristic of these discharges is also shown in Figure 4a in which a high fraction (up to 35%) of NBI current-drive and 70% total non-inductive fraction is achieved between t=0.2s and t=0.3s when the normalized density is low with Greenwald fraction ~0.4. Such parameters are approaching the parameters expected in CTF in which bootstrap and beam current drive each provide approximately half of the total current at Greenwald fraction ~0.3.

Under conditions similar to those used for achieving a high non-inductive fraction, higher plasma current and lower toroidal field were utilized to access higher normalized beta and toroidal beta at high elongation. As shown in Figure 5a, high normalized beta near 6 (red) and near the ideal-wall limit (upper grey rectangle) was accessed. As shown in Figure 5b, this was achieved at high sustained elongation κ = 2.6 - 2.7. As shown in Figure 5c between t = 0.6 and 0.75s toroidal beta of ~25% is sustained for ~3 energy confinement times before the plasma beta is transiently degraded by an n=1 MHD instability. The plasma recovers and between t=0.8s and 1s the toroidal beta reaches 27% for ~4 energy confinement times before the plasma is terminated by a large n=1 instability associated with q < 1 over much of the plasma core. Such high beta scenarios could enable a CTF to achieve enhanced neutron wall loading ~ 2MW/m^2 (versus 1MW/m^2).

Base Facility and Diagnostics Achievements for FY2009

The base facility plan was to operate the NSTX facility for 11 run weeks in FY 2009. In addition, the ARRA funding provided 5 additional run weeks making the total run weeks 16 for FY 2009. Both facility operational run week milestones were achieved ahead of schedule. A number of high priority facility and diagnostic upgrades were implemented to support the FY2009 base research plan described in the previous section. These include the dual lithium dropper system, edge sample probe, three-view divertor bolometer system, and the High-Harmonic Fast Wave (HHFW) antenna system upgrade.

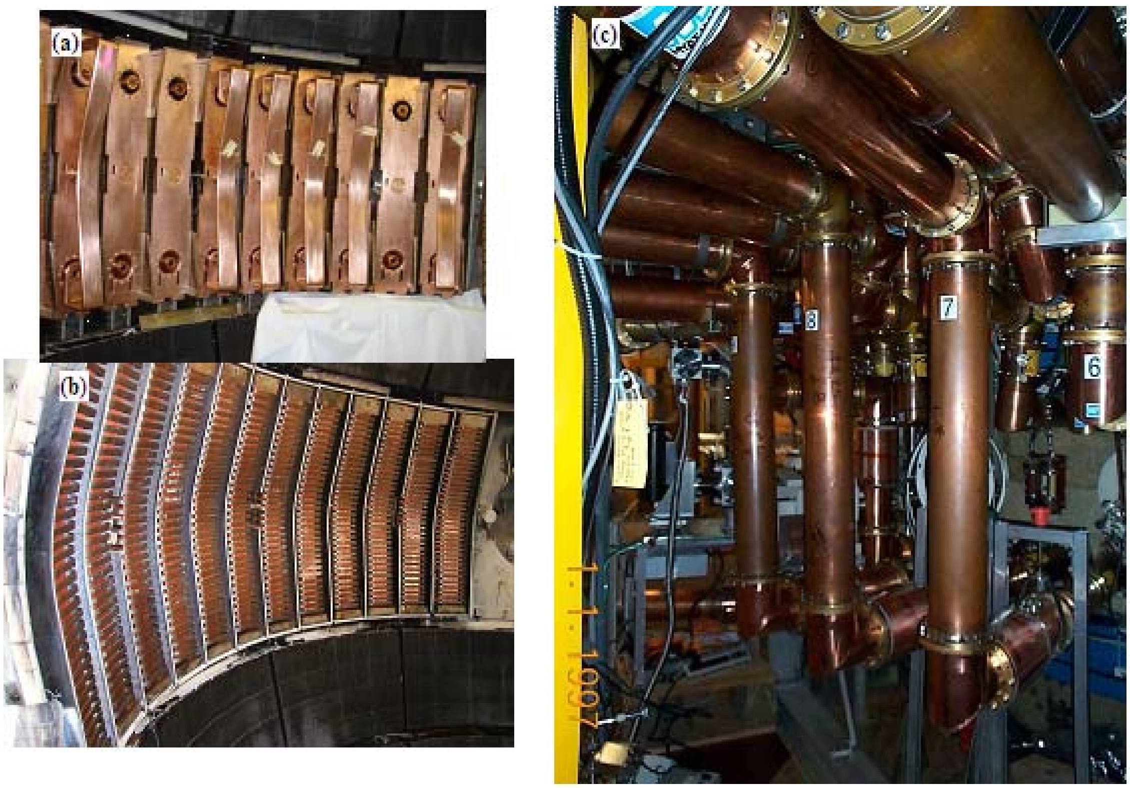

Figure 6 *- NSTX High-Harmonic Fast Wave (HHFW) Antenna Upgrade. (a) New double-feed-through (symmetric feed) antenna straps installed in NSTX, (b) new antenna with Faraday shields, and (c) resonant loops to for the double-feed-through antennas.*

The HHFW antenna system was upgraded to improve heating and current drive in H-mode discharges. The single-feed-through twelve-element antenna array was modified to a new double-feed-through (symmetric feed) configuration as showing in Figure 6a and 6b. The external loops were also installed as showing in Figure 6c. This should improve both the power handling capability and the antenna radiation pattern needed for heating H-mode discharges and for current ramp-up in FY2010.

A liquid lithium divertor (LLD) system will be installed for the FY2010 run in collaboration with Sandia National Laboratory (SNL). This will consist of a set of heated, molybdenum-coated stainless plates forming an almost continuous conical annular ring in the lower outboard divertor. When coated with lithium and heated above its melting point, the plates will provide about 7000 cm^2 of active pumping surface area in contact with the outboard scrape-off layer of the plasma. The dual LITER system installed since the FY2008 operation will be used to supply a thin layer of lithium onto the heated LLD surfaces. The ARRA funding will provide the fund to enhance the lithium delivery system and the diagnostics for the NSTX LLD.

NSTX, in collaboration with the University of Wisconsin, will be implementing a major advanced diagnostic system supported by the OFES Advanced Diagnostic Initiative. This Beam Emission Spectroscopy (BES) system will directly measure longer wavelength density fluctuations in the plasma core. Together with the existing high-k microwave tangential scattering diagnostic, which measures medium to short wavelength turbulence, BES will provide the most comprehensive turbulence diagnostic set of any ST in the world. The BES diagnostic should also be useful for measuring the spatial structure of fast-ion-driven instabilities, such as the TAE and BAAE, observed on NSTX. In FY2009, the BES system design was completed and the in-vessel components were fabricated for the installation for the FY2010 run.

In FY2009, the NSTX Upgrade Project which comprises a new center-stack and a second NBI system was initiated with the approval of CD-0 in February 2009. The conceptual design activity has started toward the CD-1 approval in FY 2010. Supporting R&D for the TF joint design and the tritium decontamination of the TFTR NBI beam box were started in FY2009.

Facility Milestones for FY2009

Facility Milestone F(09-1): Operate NSTX Facility for 11 Experimental Run Weeks (Target - September 2009. Completed – July 2009)

Milestone Report: NSTX achieved 11 run weeks with 1705 plasma shots on July 7, 2009.

Facility Milestone F(09-2): Complete fabrication of the liquid lithium divertor target for particle pumping (Target - September 2009. Completed – September 2009)

Milestone Description: Building on the results obtained with the lithium evaporator in FY2006 and 2007, the development and deployment of a liquid lithium divertor target system is proposed for NSTX. While the chemical reactivity of a solid lithium surface becomes depleted quite rapidly by plasma exposure, a liquid lithium surface can remain chemically active for continued pumping during high performance, extended discharges.

It is proposed to utilize the twin evaporator system already available on NSTX to apply thin layers of liquid lithium onto the heated divertor target surfaces. The LLD system components are being fabricated by SNL and PPPL and will be installed on NSTX during the summer of 2009 outage.

Milestone Report: The NSTX team reached an important milestone with the delivery of plates for the Liquid Lithium Divertor (LLD) being prepared for installation in NSTX in the summer of 2009 and operation in the 2010 campaign. A schematic of the LLD is shown in Figure 7a. Sandia National Laboratories has fabricated and delivered the LLD plates and the control rack to PPPL. The LLD has four 80° toroidal panels, each a conical section inclined at 22° like the previous graphite divertor tiles as shown in Figure 7a. Each LLD panel is a 22-mm-thick copper plate clad with a 0.2-mm 316-SS (brazed) and a surface layer of flame sprayed 50% porous molybdenum. This molybdenum layer will host lithium deposited from the LITER lithium evaporators in NSTX. The plates involved a challenging and complex manufacturing process. Six copper plates (including two spares) were cut, die pressed into conical sections and machined to near final shape with holes for electrical heaters and thermocouples. Subsequent steps included vacuum brazing of the thin stainless steel cladding, and vacuum flame spraying of the molybdenum coating as shown in Figures 7b and c. The LLD plates are being prepared to be installed on NSTX starting in October, 2009 to be ready for the FY2010 plasma operations starting in March 2010.

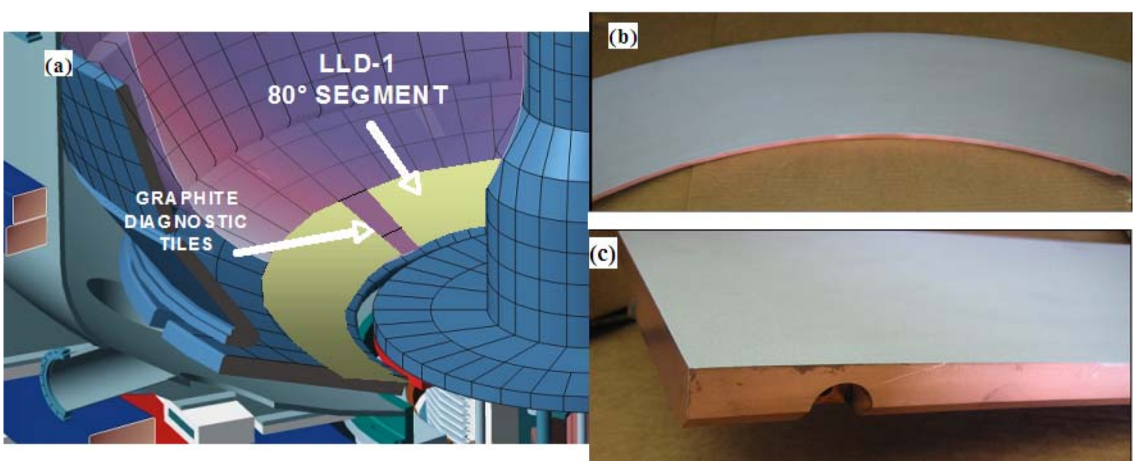

Figure 7 - NSTX Liquid Lithium Divertor Target. (a) A schematic of LLD target, (b) newly fabricated LLD plate with molybdenum coating, and (c) a close-up view of the LLD plate.

Diagnostic Milestones for FY2009

Diagnostic Milestone D(09-1): Upgrade the divertor bolometer to three views with 20 channels. (Target - September 2009. Completed – July 2009)

Milestone Description: A divertor bolometer system with a total of 20 sensors in three viewing fans in a poloidal plane as shown in Figure 8 will be completed in FY2009 to supplement the tangentially-viewing core plasma bolometer with 16 sensors. The sensors consist of a 4 μm gold foil on a mica substrate, similar to those used in JT-60, JET, and ASDEX, and have the sensitivity to measure the emission from the NSTX divertor. The vertical resolution of the inward-looking system is approximately six centimeters at the center stack. This three-view divertor bolometer system together with the tangential viewing core plasma bolometer system is intended to produce a 2D tomographic reconstruction of divertor region with good spatial and temporal resolution. This system is to be used for divertor experiments for example in which the reduction of heat-flux to the wall in a poloidally detached divertor configuration may be examined. The bolometer system was installed in NSTX during the FY2008 outage and awaiting the commissioning during the FY2009 plasma operation.

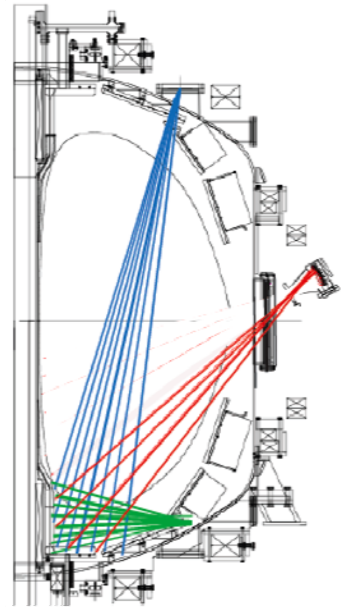

***Figure 8** - Three-view divertor bolometer*

Milestone Report: Commissioning of the new three-vew divertor bolometer diagnostic was completed during the week of July 13 after two control electronics chassis that had been repaired by the bolometer vendor were re-installed. The system took data routinely at the end of the FY2009 run and inversion software to perform tomographic reconstruction of the emission is being developed.

Diagnostic Milestone D(09-2): Complete fabrication of the Beam Emission Spectroscopy system for transport studies. (Target - September 2009. Completed – September 2009)

Milestone Description: enable direct measurements of longer wavelength density fluctuations in the plasma core providing valuable insights into the suppression of ion turbulence and the attainment of near neoclassical ion confinement on NSTX. The BES diagnostic together with the existing microwave tangential scattering diagnostic (which measures medium to short wavelength turbulence) will provide the most comprehensive turbulence diagnostic set of any ST in the world. The BES diagnostic should also enhance measurements of the spatial structure of fast-ion-driven instabilities such as the TAE and BAAE observed on NSTX. The BES system will take advantage of the research and development already performed on the DIII-D tokamak by the University of Wisconsin group. The BES system components are being fabricated by University of Wisconsin and PPPL and will be installed on NSTX during the summer of 2009 outage.

Milestone Report: Fabrication of the BES diagnostic components that will be installed inside the NSTX vacuum vessel is complete as of September 18. This includes the lenses, lens holders, and shutter mechanisms for both views. These components have been cleaned, assembled, and bench tested for optical and mechanical performance. Results of these tests were satisfactory and these assemblies are ready for installation inside the NSTX vacuum vessel. Installation started on September 21.

ARRA Facility Milestones for FY2009

ARRA Facility Milestone AF(09-1): Operate NSTX Facility for 5 Additional Experimental Run Weeks **(Target - September 2009. Completed – August 2009)**

Milestone Report: NSTX achieved 5.89 run weeks with 1705 plasma shots on August 14, 2009.

ARRA Facility Upgrades Project: The National Spherical Torus Experiment (NSTX) Research Augmentation/Upgrade Project will enable timely implementations of key, high priority NSTX facility and diagnostic upgrades which will result in significantly greater research productivity.

Project Scopes: The upgrades will allow for an upgrade to the multi-pulse Thomson scattering system for improved spatial resolution; enhance lithium liquid divertor capability for divertor pumping; increase post-doctoral staff to support enhanced research capabilities; and allow implementation of a 2nd switching power amplifier for improved error field/resistive wall mode/resonant magnetic perturbation spectra; and support completion of MSE-LIF advanced diagnostic for internal magnetic and electric field measurements.

Status: While the ARRA NSTX Facility Upgrade Project has just started in August, 2009 and there are no FY2009 milestones, the NSTX Project has made a significant progress toward the milestones in FY2010. Additional detailed plans have been laid out and engineers and designers have been assigned; the mechanical design efforts are in progress. Requisitions for key long-lead equipment have been submitted to the PPPL procurement office. One of two new post-doctoral researcher hires has begun working at PPPL and a second selected post-doc will begin work at PPPL on or before October 1, 2009.

Additional NSTX Achievements in FY 2009:

Beyond the successful completion of the FY2009 research, facility, and diagnostic milestones described above, several additional important scientific and operational results achieved during the FY2009 run are described briefly below.

ELM pacing using 3D magnetic fields: In the standard high confinement mode (H-mode) operation of a tokamak, periodic bursts of energy and particles erupt from the plasma edge due to an instability known as the edge localized mode (ELM). These ELMs have the beneficial effect of expelling excess fuel and impurities from the plasma, thereby regulating the plasma density, purity and radiated power. In future larger experiments, however, these bursts will quickly erode plasma facing components if they expel too much energy too quickly. Control of ELM size can be achieved by either instigating higher frequency, small ELMs ("ELM pacing"), or by developing ELM-free scenarios with steady-state means to expel impurities and prevent pollution of the core plasma. Over the past few years, the application of small 3D (non-axisymmetric) magnetic field perturbations has been used in the DIII-D tokamak to eliminate ELMs and reduce impurity accumulation by increasing the particle transport at the plasma edge. However, the physics of how 3D fields affect transport at the plasma edge is not yet well understood, and recent experiments performed in NSTX routinely observe ELMs to be triggered by 3D fields rather than stabilized. In a different set of experiments, it was found that lithium wall coatings can stabilize ELMs and produce plasma confinement that

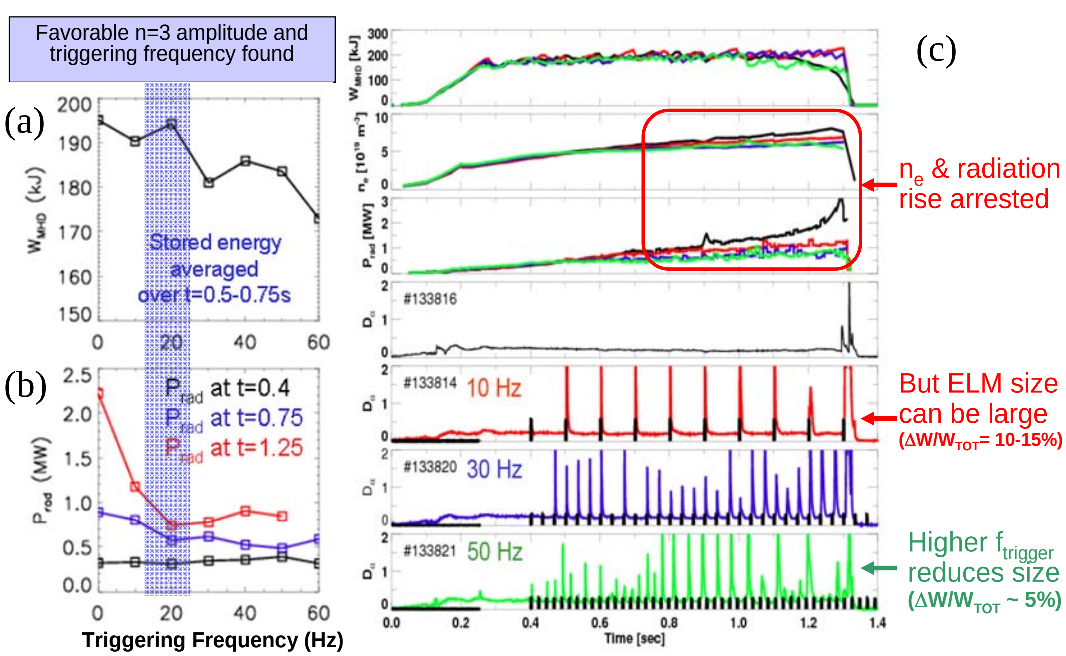

***Figure 9** - (a) Stored energy change from an ELM vs. ELM triggering frequency, (b) radiated power at different times during plasma vs. ELM triggering frequency, and (c) time-histories of discharge parameters for 3 different triggering frequencies (10, 30, 50Hz).*

is so high that impurities accumulate resulting in plasma termination due to impurity radiation. The combination of ELM pacing with periodic pulses of 3D fields added to the lithium-enhanced discharges has been shown to be effective at preventing impurity accumulation while retaining the high confinement characteristics achieved with lithium coatings. Recent efforts have doubled the frequency and increased the reliability (increased from 50-75% to 100%) of the ELM pacing, towards the goal of triggering rapid, small ELMs in both ELM-free and large-ELM plasmas. The results of this optimization are shown in Figure 9. Figures 9a and 9b show that for a favorable pacing frequency of 30Hz the stored energy decrement from ELM pacing is small while the radiated power late in the plasma (t=1.25s) can be reduced by a factor of 3. As shown in Figure 9c, by increasing the triggering frequency to 50Hz (bottom plot), the ELM size, expressed as the fraction of plasma energy lost at each ELM, can be reduced from 10-15% down to 5%. Further optimization of ELM pacing is being actively pursued to reduce the size of triggered ELMs sufficiently to be acceptable in future experiments. These experiments are providing new techniques and understanding for controlling edge transport to optimize fusion performance.

Improved coupling of Coaxial Helicity Injection (CHI) to induction: In FY2008, up to 50kA of CHI non-inductive start-up current was coupled to inductive ramp-up plasmas which when heated with NBI achieved plasma temperatures over 800eV and accessed H-mode confinement. Importantly, these experiments demonstrated the compatibility of CHI start-up with subsequent high-performance plasma operation. However, these CHI experiments were limited by impurity production in the divertor region and by absorber arcs. In FY2009, extensive conditioning of the divertor region enabled greatly reduced impurity production during CHI. Further, by energizing the previously installed absorber nulling coils, it was found that a rapid ramp of absorber coil current could help push the plasma downward (away from the upper insulating gap) during the rapid expansion phase of the plasma. This modification to the poloidal field evolution during CHI ramp-up kept the plasma from reaching the absorber gap thereby avoiding/delaying absorber arcs.

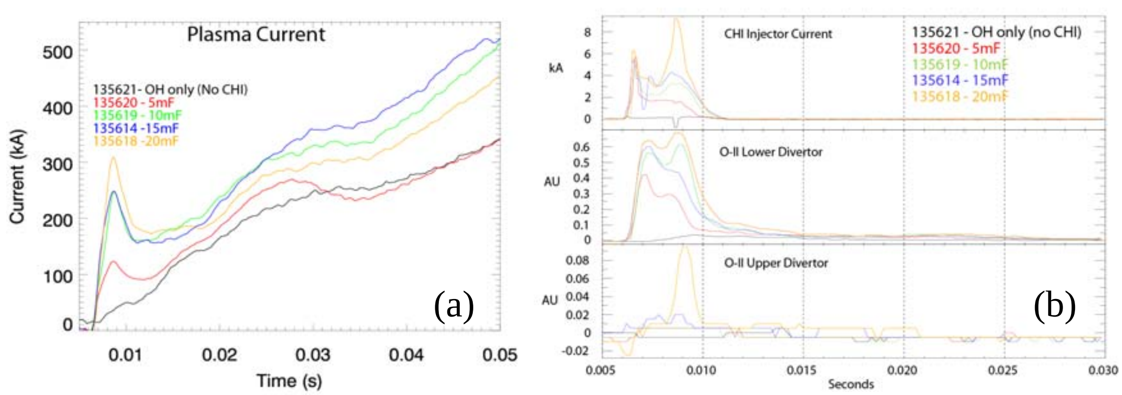

__Figure 10 -__ (a) Plasma current evolution during experiments coupling CHI to induction vs. capacitor bank capacitance (proportional to CHI start-up energy) and (b) CHI injector current and oxygen impurity evolution in the lower and upper divertors.

These combined improvements increased the current coupled from CHI to induction by a factor of 3-4 to nearly 200kA. As shown in Figure 10a, the plasma current at t=50ms increased from 340kA with induction only (black) to 520kA (blue) with 15mF of CHI bank capacitance. This represents a poloidal flux saving equivalent to 180kA of plasma current which is ~25% of the nominal operating current of 700kA long-pulse operating scenarios on NSTX. As shown in Figure 10b, when the capacitance is increased to 20mF, thereby proportionally increasing the energy supplied, a “spike” on the CHI current is observed around 8ms. The lower graph of the same plot shows that the upper oxygen radiation occurs at the same time which is indicative of an absorber arc. Thus, further optimization of the absorber-region poloidal field is needed to avoid absorber arcs at higher CHI start-up energy. If absorber arcs can be avoided, 300kA or higher start-up current is projected to achievable. Such current levels project to ~1MA or more of current in an ST-CTF and indicate that CHI could be an important tool for non-inductive start-up in next-step STs.

Improved high-harmonic fast-wave heating performance and understanding:

The upgraded NSTX HHFW heating system was utilized in the later part of the FY2009 run to test the performance of the upgrade and to support transport experiments. After antenna conditioning, the HHFW performance quickly matched and then exceeded previous performance. As shown in Figure 11, the peak central electron temperature reached 5.7keV near t=0.3s with an RF heating power of 2.7MW. This compares favorably with the previous record of 5keV using 3.1MW of heating power representing a 30% increase in heating efficiency. More importantly, heating to central electron temperatures of 3.5-5keV at 2.7MW was sustained for 0.3s which represents a record NSTX duration at this high sustained central electron temperature. Additional antenna conditioning and modest improvements to the external RF circuitry are expected to increase the sustainable RF heating power to at least 4MW in FY2010.

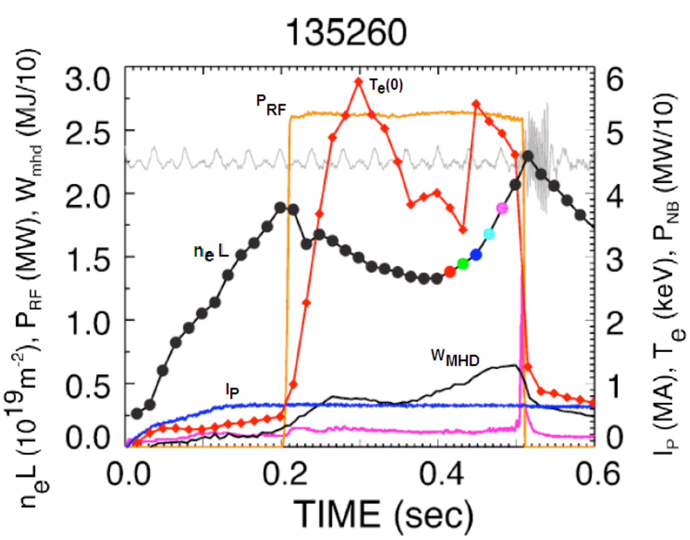

***Figure 11** – Time histories of plasma parameters during HHFW heating of a helium plasma using the upgraded antenna system.*

Progress in understanding the interaction between the NBI fast-ions and HHFW fast-ion-acceleration was also achieved in FY2009. Changes in the fast-ion density profile during

HHFW heating have been measured with the FIDA diagnostics for the first time in NSTX. Figure 12a shows the measured increase in fast-ion density for the effective ion energy range E_λ = 30 to 60keV which is induced by HHFW acceleration of fast-ions from lower to higher energy. As shown in Figure 12b, the largest relative increase in fast-ion density for this energy range is a factor of 3-4 and occurs in the plasma core near the 7th and 8th deuterium cyclotron harmonic layers. Relative density increases of 1.5-2 are also observed over most of the plasma minor radius including near the plasma edge at the 11th cyclotron harmonic.

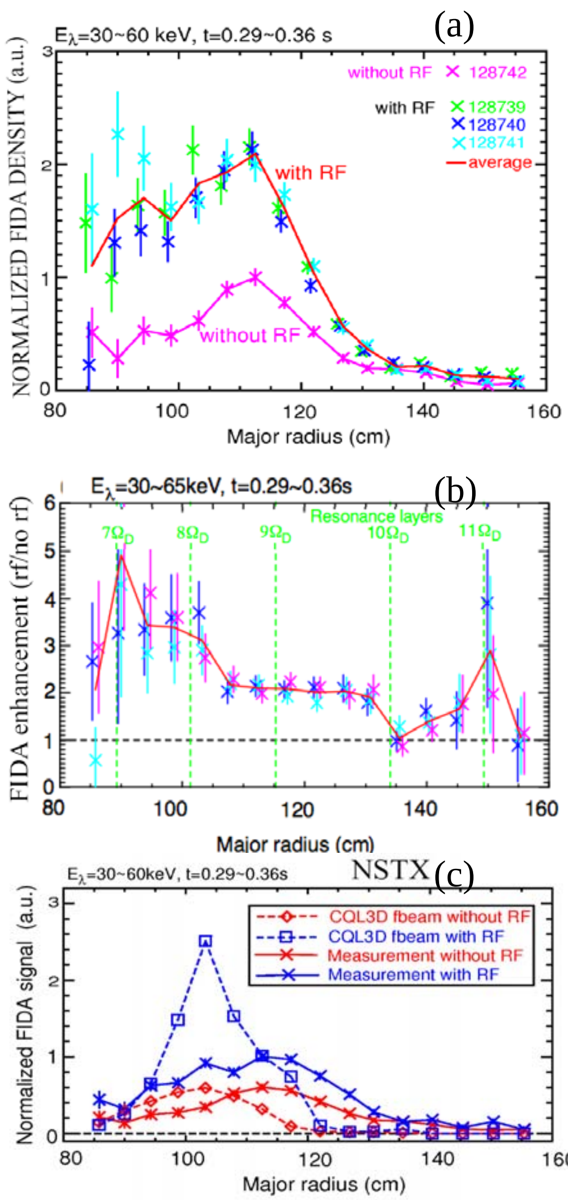

***Figure 12** – (a) NBI fast-ion density profiles with and without HHFW heating, (b) enhancement ratio of fast ion density profile – RF/no-RF, and (c) comparison between measured and predicted (CQL3D) fast-ion density profiles with and without RF.*

Figure 12c compares the measured to predicted (using the CQL3D code) FIDA signals for a plasma with NBI-only (no RF) and with NBI+RF. As is evident from the figure, the measured density profiles without RF are significantly broader than the code prediction, and peak near 110-115cm (measured) vs. near 100-105cm (prediction). The difference between measured and predicted profile shape is even more apparent for the cases with RF, as the peak predicted density is 3 times higher than the measured value and is again inwardly shifted. The cause of this discrepancy is very likely the approximation of zero ion banana width used in CQL3D which is a poor approximation in NSTX in which the fast-ion banana widths range from 10-15cm. Finite banana width effects are actively being incorporated into the CQL3D and AORSA RF codes to improve the models and to enable better predictive capability for fast-ion interactions with the HHFW in NSTX.

NSTX Research in Support of ITER:

The elimination and/or reduction of the size of edge localized modes (ELMs) is a high priority research area for ITER to support high-confinement H-mode operation while protecting the ITER divertor. The contributions from NSTX to this area via ELM triggering have been described above. Another related high priority research for ITER is the L-mode to H-mode power threshold – in particular the species dependence of the threshold since initial ITER operation will be carried out in either H or He. Several NSTX experiments were carried out in the transport topical science group to better understand the broad parametric dependencies of the H-mode power threshold for both STs and tokamaks.

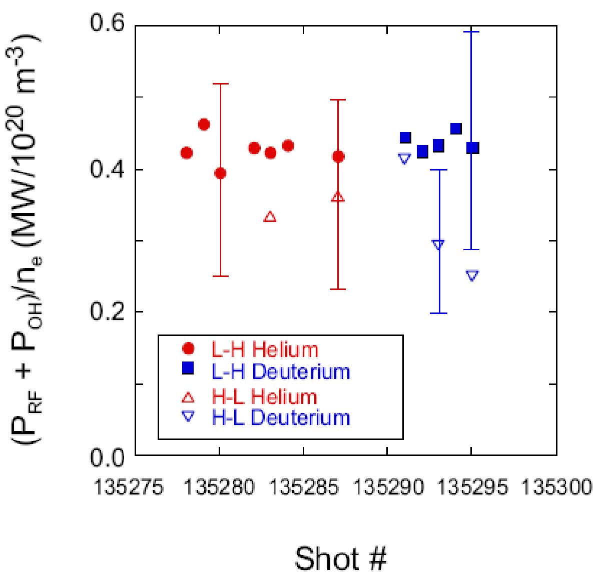

***Figure 13** - H-mode threshold powers for L-H and H-L back transitions as a function of plasma main-ion species deuterium and helium.*

First, we note that previous scaling studies have shown a nearly linear dependence of threshold on density, so the threshold power P_{LH} is normalized to the line-average density n_e in the discussions below. Figure 13 shows the most important result from the H-mode threshold scans in NSTX. As is evident from the figure, the density-normalized helium L→H threshold powers (red circles) are nearly identical to the deuterium threshold powers (blue squares). Since results from other experiments have shown that hydrogen plasmas may have threshold powers nearly twice as high as for deuterium, the NSTX results indicate that operation in He may be the best approach to developing H-mode scenarios in the early operation of ITER. As in other devices, hysteresis in the threshold power is also observed in NSTX, and Figure 13 shows that the power for an H→L back-transition is approximately 20-30% lower than the power for the initial L→H transition.

Additional experiments were performed to measure the dependence of the L→H transition on 3D magnetic fields and rotation. These experiments were motivated by JET ripple experiments which showed a strong dependence on ripple strength, and by DIII-D NBI torque scan experiments. Recent NSTX and MAST experiments exhibited delays in the H-mode transition with increasing applied field amplitude, and in NSTX n=3 magnetic braking was used to change rotation and assess the effect on threshold power. It was found that P_{LH}/n_e is significantly higher (65% higher) with higher applied n=3.

The difference in rotation does not appear to be the dominant change in these studies – consistent with earlier RF versus NBI threshold experiments. Finally, the dependence of H-mode threshold on plasma current and lithiumization was studied. For the current dependence, it was found that P_{LH}/n_e was almost a factor of 2 higher for 1MA plasma current than for 0.7 MA - indicating a very strong dependence on plasma current. For the lithiumization dependence, lithium divertor/wall conditioning was found to reduce the power threshold by 30-40% with P_{LH}/n_e ~ 0.9 MW/10^{19}m^{-3} (2.7MW NBI) without Li evaporation versus P_{LH}/n_e ~ 0.6 MW/10^{19}m^{-3} with Li evaporation (1.4MW NBI).